Geomagnetic Field Based Indoor Localization Using Recurrent Neural Networks

Ho Jun Jang, Jae Min Shin and Lynn Choi
School of Electrical Engineering
Korea University
Seoul, Korea
{nametom, neo_power, lchoi }@korea.ac.kr

***Abstract*- The time-varying, unstable nature of RF signals has limited the accuracy of RF-based indoor positioning techniques such as Wi-Fi fingerprinting. Positioning errors of over 10 meters are reported in large-scale indoor environment such as airport and department stores. Compared to RF or ultrasound signals, the geomagnetic field signal exhibits stable signal strength in time domain. However, the existing geomagnetic field based indoor localization still relies on the fingerprinting technique, which is borrowed from the RF-based indoor positioning. This cannot resolve the distribution of the same geomagnetic field values and thus became a major reason for diminished performance of geomagnetic-based indoor localization. In this paper, we propose a novel indoor localization technique that uses magnetometer sensor readings as input to the artificial neural network models. The idea is that although there can be multiple locations having the same magnetic field value, as a pedestrian moves the sequence of magnetic field values will lead to a unique pattern of the sensor readings over time. We use a recurrent neural network (RNN) since it can characterize a particular location based on the current input as well as the past sequence of inputs. We first build a geomagnetic field map on our campus test-bed. Then, we generate a million traces of various pedestrian walking patterns from the map. We use Google Tensorflow with NVIDIA cuDNN library as a Deep Learning framework. 95% of the traces are used for training and 5% of the traces are used for localization evaluation. In this preliminary evaluation, we show an average positioning error of 1.062 meters compared to the average error of 3.14 meters of our BLE fingerprinting results. We cannot only improve the localization accuracy but we are also able to address the problem of continuous route tracking, which was not possible with the RF-based fingerprinting.**

Keywords – Indoor Localization, Geomagnetic Field, Deep Learning, Recurrent Neural Network, Object Tracking

I. INTRODUCTION

With the rapid proliferation of smart phones, commercial interests and demand for indoor location-based services (LBS) such as shop advertisements, indoor navigation, museum guides, augmented reality, and disaster rescue, are quickly increasing. Since most of these LBS applications like asset tracking and indoor navigation often require more fine-grained positioning accuracy in indoor than outdoor environment, an accurate and economical solution for indoor positioning is a key enabling technology for LBS. There is a diverse range of indoor localization techniques [1], which can be classified into RF signal-based, image-based or sensor-based. Among them, RF signal-based systems are the most common since widespread network devices make them easily deployable and the system guarantees reasonable performance with affordable cost. Since the introduction of Microsoft's RADAR [2], academic research of indoor localization primarily focused on RF signal-based systems.

RADAR introduced Wi-Fi fingerprinting which compares the received signal strength (RSS) of the RF signal at a particular location with the pre-recorded RSS values of reference points by using the K-Nearest Neighbor algorithm to determine the relative proximity of the location with the reference points. Since then, various RF signal-based fingerprinting techniques have been studied using WLAN [2, 3], RFID [4], Bluetooth [5, 6], and GSM [7] as shown in Table 1. However, the existing RF fingerprinting schemes exhibit significant variations in positioning accuracy. This can be attributed to the unstable nature of RF signals in time domain, which is caused by interference, diffraction, and reflection of RF signals in indoor environment. A recent study [8] reports positioning errors of over 10 meters in large-scale indoor

TABLE I. Comparison of RF-based indoor positioning methods.

System / Solution	Wireless Technology	Positioning algorithm	Accuracy	Testbed scale
Microsoft RADAR [2][3]	WLAN(RSS)	K-NN	3~5m	22x43m
DIT [9][10]	WLAN(RSS)	MLP, SVM	~3m	30x25m
Hours [11][12]	WLAN(RSS)	Probabilistic method	~3m	68x25m
LANDMARC [4]	Active RFID(RSS)	K-NN	~2m	Small Scale
TOPAZ [6]	Bluetooth(RSS) + IR	Nearest tag	~2m	Small Scale
Robot-based [13][14]	WLAN(RSS)	Bayesian approach	~1.5m	32x17m
GSM Fingerprinting [7]	GSM cellular network(RSS)	K-NN	~5m	88x113m

978-1-5090-5019-2/17/$31.00 ©2017 IEEE

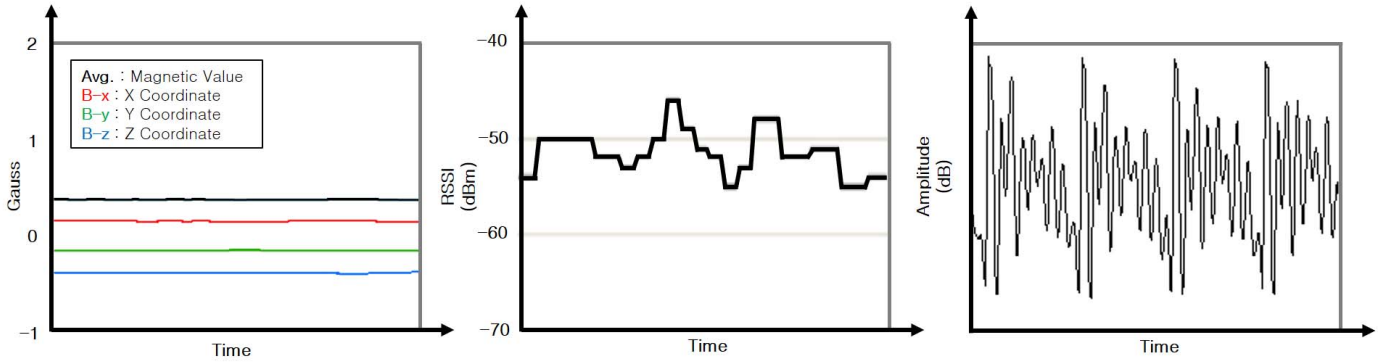

Fig. 1. Measurements of geomagnetic field, wireless LAN, and sound waves according to time

environment such as airports and department stores. Therefore, RF signal-based fingerprinting does not fulfill the performance requirement of indoor LBS applications.

Most of the existing RF signal-based indoor localization techniques including fingerprinting, time of arrival (ToA), and time difference of arrival (TDoA), compute single individual position at a time based on RSS or flight time of the RF signals. Therefore, each indoor positioning produces an absolute position result but each result does not have any relationship with previous result. Due to its poor positioning accuracy, the existing RF signal-based indoor positioning leads to irregular tracking routes when individual results are combined for continuous tracking.

In this paper, we propose a new indoor localization algorithm, which is fundamentally different from the existing solutions in the following aspects. First, we use geomagnetic field signal, which is quite stable in time domain as opposed to RF signal or sound waves as shown in Figure 1. Second, we no longer rely on fingerprinting to estimate the current position. Although geomagnetic field has been used for indoor localization [15], most of the existing studies still rely on fingerprinting, which cannot resolve the distribution problem of the same magnetic field values. Third, our proposed scheme is a positioning scheme that the current position is determined based not only on the current geomagnetic field value but also on the past geomagnetic field values. Thus, we could produce smooth and contiguous tracking routes for indoor tracking and navigation. Finally, we employ deep learning techniques to identify the unique changing pattern of the geomagnetic field values that the pedestrian movement creates and to improve the accuracy of indoor positioning. Specifically, we train recurrent neural network (RNN) model to memorize the geomagnetic field map of indoor environment and use the trained model to predict the current location of the pedestrian.

To evaluate our geomagnetic indoor localization scheme based on RNN model, we build a campus test-bed that can test both geomagnetic field localization and Bluetooth Low Energy (BLE) fingerprinting. We build both geomagnetic field map and radio map with 629 reference points that are spaced every 57cm interval in the testbed of 21.47 meters by 10.17 meters area. From the geomagnetic field map, we generate a million traces of various pedestrian walking patterns. 95% of the traces are used for training the RNN model while the remaining 5% of the traces are used for evaluation. With the supervised neural network training that consists of feed-forward computation of inputs and weights, and the back-propagation of mean squares of localization errors, we construct an optimized recurrent neural network model for the test-bed by varying the mini-batch size and the number of hidden nodes through repeated experiments. From the evaluation, we could achieve an average localization error of 1.062 meters and the maximum error of 3.874 meters for the test-bed. As we increase the number of hidden nodes, we could generally improve the localization accuracy. However, we observe a minor increase in the localization error as well as in the variance of the errors when the number of hidden nodes exceeds 200. In conclusion, compared to the traditional RF signal-based indoor localization we could not only improve the absolute indoor localization accuracy but also we could produce a more accurate and continuous tracking routes for indoor object tracking.

In the following, we first discuss the background and motivation of our work in Section II. Then in Section III, we present our proposed RNN model and explain how we apply the RNN model for indoor localization. In the section, we also discuss how we construct the geomagnetic field map for our test-bed and how we could generate training and evaluation traces from the map. In Section IV, we evaluate the localization performance of our proposed RNN-based indoor localization scheme by varying the number of hidden nodes as well as the mini-batch size. Finally, in Section V we conclude the paper and discuss our future work.

II. BACKGROUND

In general, indoor positioning techniques can be classified into absolute positioning techniques and relative positioning techniques. RF signal-based technique is an absolute positioning technique where the estimated location is derived from the current RF signal strengths but it is independent of previous RF signal strengths. According to Friis' transmission equation [16], the strength of an RF signal quadratically diminishes as the signal traverses from the originating source of the signal.

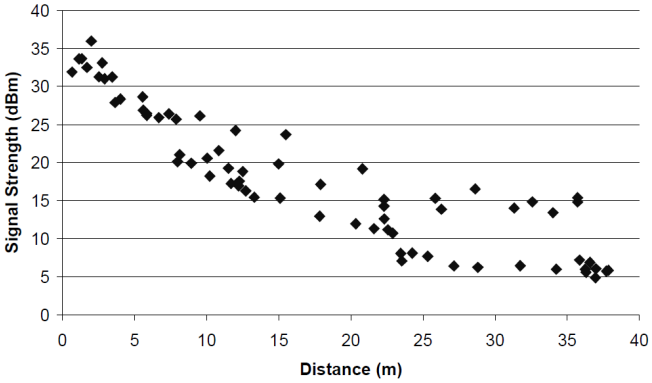

Fig. 2. Irregular degradation of signal strength over distance [2]

Ideally, we can estimate the distance from the source by measuring the signal strength if we know the original signal strength and its attenuation assuming an ideal empty space. However, in indoor environment, the signal strength varies irregularly, as it gets further away from the radio transmitter

as shown in Figure 2 due to phenomena such as reflection, diffraction, and interference. The irregularity becomes the main cause for the inaccuracy of the existing RF signal-based indoor localization techniques [8]. RF signal-based indoor localization algorithms [2, 3, 4, 5, 6, 7] focus on improving the accuracy of localization in singular position regardless of previous positions. As there is no correlation between each indoor localization result and due to the inaccuracy of the current localization techniques, it makes it quite difficult to produce a smooth and contiguous route of a moving object in indoor tracking.

The Pedestrian Dead Reckoning (PDR) estimates the movement of a pedestrian, more specifically the step count and orientation of the movement by using the IMU sensor. Compared to RF signal-based techniques it is a relative positioning technique in that it calculates the next position relative to the current position. This leads to incremental and contiguous location tracking which is not possible with the current RF signal-based localization schemes. However, it can only provide a relative positioning result. Without knowing the current absolute location, its positioning result can be expressed only relative to the unknown starting point. Furthermore, the localization error of PDR increases over time due to the accumulating error caused by the inaccuracy of the IMU sensor and the PDR algorithm.

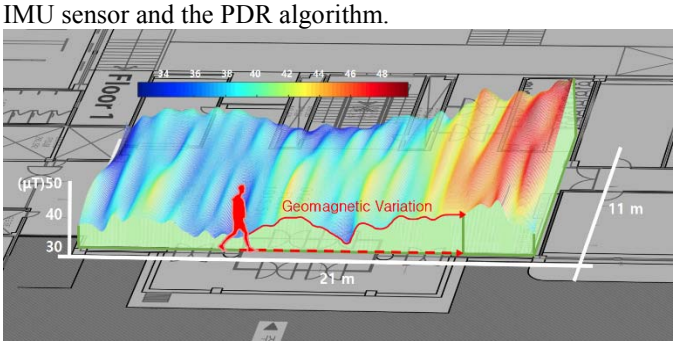

Fig. 3. Geomagnetic field variation according to movement

Although indoor localization schemes [15] based on the geomagnetic field sensor exist, they still rely on the algorithm derived from RF-based fingerprinting. Like Wi-Fi fingerprinting, they also construct a geomagnetic field map that measures the geomagnetic sensor values at predetermined reference points. After measuring the geomagnetic sensor value at a certain unknown position, the existing scheme compares the value with those of the reference points in the map. By computing the Euclidean distance among the values with K-NN (Nearest Neighbor) algorithm, it finds the closest K neighbors and estimates the location that is actually the weighted center of those K neighbors. However, as shown in Figure 3 and Figure 5 there can be many different locations with the same magnetic field value in the map. Therefore, it may lead to an inaccurate positioning result. To resolve the problem, Magicol [17] proposed that instead of traditional geomagnetic field map that contains a magnetic field value at each reference point, they create and manage a new table whose entry records magnetic field value variations created by each movement. After they detect a sequence of magnetic field values, they compare the sequence with the entries in the table. If they find a similar pattern in the table, they report the coordinate mapped to the pattern as a localization result, avoiding the problem of distribution of the same magnetic field value in the previous magnetic map. However, the method still has the drawback that it cannot provide localization service in areas where the information of the pattern is not pre-inputted. In addition, the time to collect preliminary data is significant compared to general magnetic field maps and the process is more complicated.

III. SYSTEM DESIGN

A. Geomagnetic Field Map

The geomagnetic field is a massive magnetic field flow created by the Earth's internal activity. The Republic of Korea is positioned in the 50μT (micro Tesla) zone [18]. In indoor environment, the geomagnetic field is distorted by various structures inside buildings such as steel structures, steel shelter doors, elevators, and generators. This creates a distribution of a wider range of geomagnetic field values in indoor than in outdoor environment. The geomagnetic field values can be measured through the Geomagnetic Hall Effect [19] using smart phone magnetic field sensors or standalone magnetic field sensors as illustrated in Figure 4.

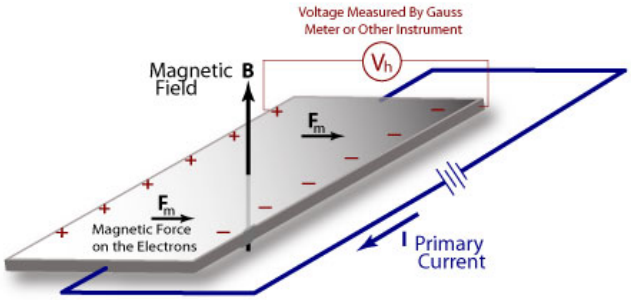

Fig. 4. Geomagnetic Hall Effect [19]

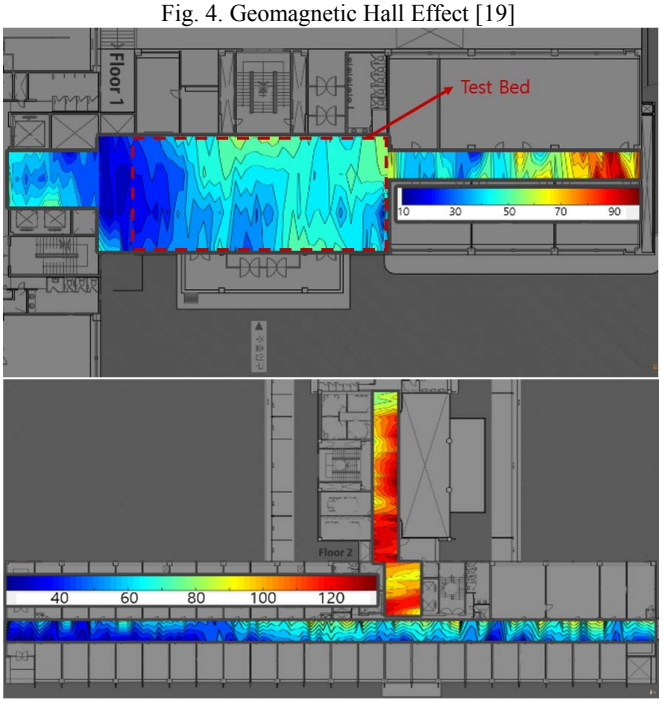

Fig. 5. Geomagnetic field maps of the first and the second floor in the College of Engineering Building at Korea University

We first build a geomagnetic field map on our campus test-bed, which spans the area of 21.47 meters by 10.17 meters on the lobby of our College of Engineering building as shown in Figure 5. We collect geomagnetic sensor data every 57cm interval and create 629 reference points in the intersections of grid-layout in the map. To improve the resolution of the geomagnetic map, we divide each 57cm interval into five 11.4cm interval and create 14661 final reference points using linear interpolation. Figure 6 shows the simplified view of magnetic field map creation process where we store the map into the map DB. We use the geomagnetic field sensor embedded in the IMU sensor of an Android smartphone to

measure the magnetic field value vector at the reference points. Figure 5 shows a graphic visualization of the geomagnetic field map mapped to the actual indoor map of our test-bed.

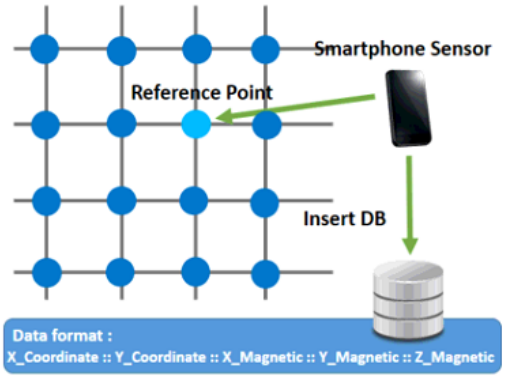

Fig. 6. Geomagnetic field creation process

B. Recurrent Neural Network model

A recurrent neural network (RNN) is a class of artificial deep neural network where connections between units form a directed cycle. Therefore, the output results learned with a RNN model have the characteristic of being determined not only by the current input value but also by all of the previous input values. Thus, RNN is often used in the situations where input and output data have a continuous relationship with time. Figure 7 shows the structure of a basic RNN model.

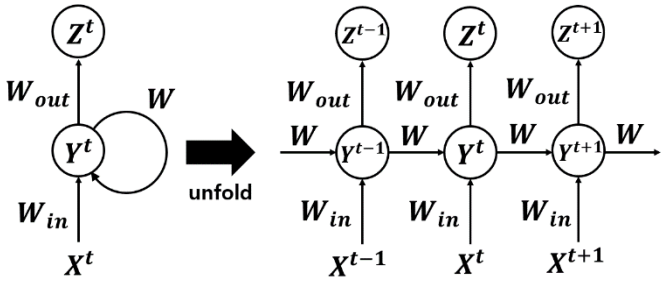

Fig. 7. The structure of a basic Recurrent Neural Network

A geomagnetic sensor measures the geomagnetic field values in the form of 3-dimensional field vector, which is used as an input to the basic RNN model. We express the input vector at time **t** as ($\mathbf{X_1^t}$, $\mathbf{X_2^t}$, $\mathbf{X_3^t}$) while the output of hidden node as $\mathbf{Y^t}$ and the final output as a 2-dimensional vector ($\mathbf{Z_1^t}$, $\mathbf{Z_2^t}$) in space. We vary the number of hidden nodes from 10 to 200 to find an optimized RNN model in our evaluation. We denote weights applied to the links from input nodes to hidden nodes, hidden nodes to hidden nodes, and hidden nodes to output nodes as $\mathbf{W_{in}}$, $\mathbf{W}$ and $\mathbf{W_{out}}$ respectively. If we express the activation function of a hidden node as **f**, and the activation function of an output node as $\mathbf{f_{out}}$, then we can define the output $\mathbf{Z_j^t}$ of the RNN model at time **t** as follows:

$$\mathbf{Z_j^t = f_{out}(W_{out}(f(W_{in}X_i^t + WY^{t-1}))}\ (\mathbf{i} \in \{1, 2, 3\}, \mathbf{j} \in \{1, 2\})$$

Although RF-based fingerprinting is vulnerable to the distribution of the same received signal strength in multiple indoor locations, it can alleviate the problem with SSID since an RF signal can reach a certain range depending on its transmission power. As opposed to the RF-based fingerprinting [15], techniques using the geomagnetic field could not resolve the problem of differentiating the same geomagnetic field value registered at multiple locations, which could potentially degrade the performance of the geomagnetic field based indoor localization. However, in this paper we can differentiate the locations with the same magnetic value into distinctive locations by training the deep neural network to memorize the changing pattern of geomagnetic value sequence instead of a single value.

C. Data Generation for Training and Evaluation

We use the geomagnetic field map to generate training and evaluation data. To generate input and output data for supervised training, we model the movement of a pedestrian using a modified version of the random way point model [20] where a user moves a certain number of steps into one direction, pauses, and change direction and moves another number of steps into that direction, and continues. The movement is confined in the geomagnetic field map. We use the geomagnetic field vector at each step as an input vector while the 2-dimensional coordinates of the corresponding location as output. The total distance of the movement path is approximately 570 kilometers. The path consists of 1,000,000 continuous steps (coordinates) and the data size is 67.9MB. We use 20-step movement as a single input trace for training. Therefore, we have 50,000 traces for both training and evaluation. Figure 8 shows a sample of the experimental data.

```
x: 49.981627, y: 74.809191 / x: -12.840187, y: -25.661308, z: -37.471752
x: 50.963254, y: 74.618382 / x: -12.794736, y: -25.671062, z: -36.950087
x: 51.944882, y: 74.427573 / x: -12.737921, y: -25.678593, z: -36.445588
x: 52.926509, y: 74.236764 / x: -12.670318, y: -25.686124, z: -35.968060
x: 53.908136, y: 74.045955 / x: -12.591925, y: -25.693655, z: -35.517505
x: 54.889763, y: 73.855146 / x: -12.502744, y: -25.701187, z: -35.093921
x: 55.871390, y: 73.664337 / x: -12.657172, y: -25.664741, z: -34.612866
x: 56.853017, y: 73.473528 / x: -12.824508, y: -25.612549, z: -34.131976
x: 57.834645, y: 73.282719 / x: -12.972065, y: -25.549569, z: -33.660976
x: 58.816272, y: 73.091910 / x: -13.099843, y: -25.475800, z: -33.199866
x: 59.797899, y: 72.901101 / x: -13.207841, y: -25.391242, z: -32.748646
x: 60.779526, y: 72.710292 / x: -13.118590, y: -25.061164, z: -32.538463
x: 61.761153, y: 72.519483 / x: -12.991776, y: -24.680408, z: -32.394065
x: 62.742781, y: 72.328674 / x: -12.876650, y: -24.312239, z: -32.255061
x: 63.724408, y: 72.137865 / x: -12.773212, y: -23.956657, z: -32.121451
x: 64.706035, y: 71.947056 / x: -12.681461, y: -23.613662, z: -31.993236
```

Fig. 8. Experimental data sample

For this study, 95% of this experiment data, or 950,000 continuous coordinates, are used for training while the remaining 5% are used for evaluation. Differentiated by the backslash (/) in Figure 8, the **x, y** values on the left are the coordinates where 1 unit corresponds to 11.4 cm of the actual space and the **x, y, z** values on the right are the 3-dimensional magnetic field vector values mapped to each coordinate in magnetic field units (μT).

IV. EVALUATION

A. Experimentation

Table 2 shows our machine configuration and deep learning frameworks used for our experimentation.

TABLE II. Experimentation Environment

Category	Machine / Tools
CPU	Intel i7-6900K 3.2GHz (8C16T)
GPU	NVIDIA Geforce GTX1080 8GB
RAM	DDR3 32GB 2133MHz
OS	Ubuntu Server 16.04 LTS
Language	Python 3.5
Library	Google Tensorflow 1.2 NVIDIA cuDNN v5.1

Numerous deep learning frameworks are available. Among them, we chose Google Tensorflow, which is provided as a framework, not as an application. This allows us to design an artificial neural network model in more detail. By using NVDIA cuDNN library and CUDA GPU parallel processing, we could improve the training performance by four times on average.

B. Neural Network Training

We trained RNN with input and output data generated from the geomagnetic field map. In the artificial neural network

training process, the number of hidden nodes, mini-batch size, the total number of execution epochs (iterations over entire dataset), and learning rate are important parameters affecting the training performance. We vary all of these parameters to find an optimized RNN model for the test-bed. We initialize biases and weights using a standard normal distribution. We use Adam as the optimizer and MSE (mean square error) as the loss function. Through repeated feed-forward propagation of inputs and weights and back propagation of errors, we optimize the weights as well as the other configuration parameters.

Figure 9 shows the average localization error during the training in terms of epoch count as we vary the number of hidden nodes from 10 to 50, 100 and 200 with mini-batch size of 20 over three iterations of the entire experiment process. As we increase the number of hidden nodes, the training time to reach a target localization error diminishes. With 200 hidden nodes, the trained RNN model can produce an average localization error of less than 2 meters in just 40 epochs while RNN model with 10 nodes cannot reach the same localization accuracy with more number of epochs.

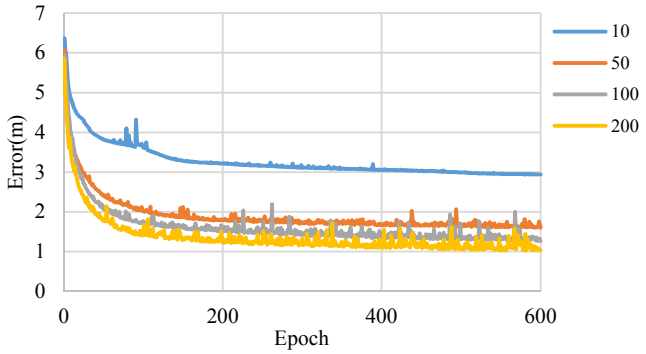

Fig. 9. Localization error of training data in terms of the number of hidden nodes

If we train an artificial neural network model by using the whole dataset configured as a single batch, the model will soon forget the first data learned and there is a strong possibility that the gradient explosion would occur as the iteration of the neural network training increases. In addition, due to the structural characteristic of Tensorflow framework, a memory shortage problem usually occurs during the training since we must configure the entire neural network model for the batch in advance to conduct the experiment. In order to resolve the problem, we reconfigure the entire dataset into many small sub-datasets called *mini-batch*. We also conduct batch normalization [21] in order to train the model with each mini-batch data set more efficiently. Figure 10 shows the average localization error during the training process as we vary the mini-batch size assuming 200 hidden nodes. In the figure, each graph is the average result of three experiments. As shown in the figure, as we increase the mini-batch size, it seems like that training takes longer. However, it is actually the number of 'epochs' rather than the 'real time'. Since larger mini-batch can process more data per mini-batch, we can reduce the 'real training time' as we increase the mini-batch size. In fact, we can substantially reduce the training time with mini-batch size of 500 compared to mini-batch size of 20 or 100. However, a large size mini-batch such as 500 cannot reach a localization error below 1.5-meter accuracy even at 600 epochs while smaller size mini-batch such as 20 or 100 can. In the figure, mini-batch size of 20 gives the best overall performance.

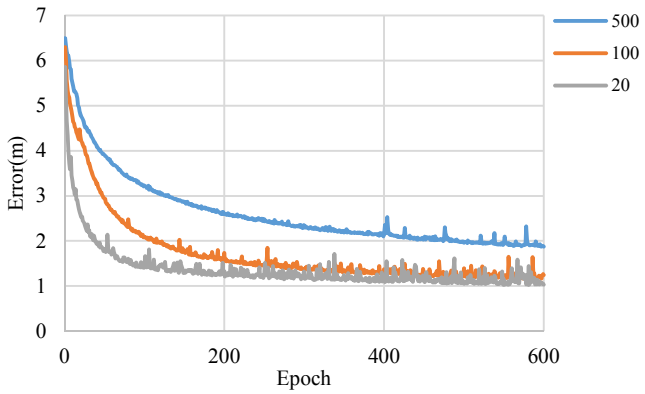

Fig. 10. Localization error of training data in terms of mini-batch size

Table 3 shows the configuration of the final RNN model optimized from the training data and other training parameters we have selected.

TABLE III. Experiment Setup

Category	**Value**
Neural model	Recurrent Neural Network
Loss function	Mean Squared Error (MSE)
Optimizer	Adam
Hidden node	200
Learning Rate	0.001
Mini-batch size	20

C. Evaluation

By using 50,000 coordinates and their corresponding geomagnetic vectors that model various pedestrian movement traces generated from the geomagnetic map, we evaluate the localization accuracy of the trained RNN model. Figure 11 shows the distribution of the localization errors for the entire evaluation data set. We could achieve the localization error of 1.062 meters when we average over three experiments. Note that this is simply the localization accuracy from the evaluation data rather than the actual measurement. The minimum error observed is 0.441 meters while the maximum error is 3.874 meters.

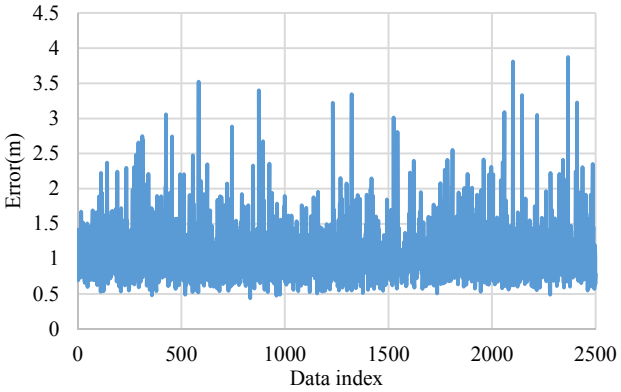

Fig. 11. Distribution of localization errors for the entire data set

Figure 12 shows the visualization of both original and predicted paths for a sample movement. The red dot is the starting point of the original path while the green dot is the starting point of the predicted path. We can see that the RNN-based path prediction can produce a quite accurate yet smooth movement path for the indoor tracking, which may not be achievable with the existing RF-based indoor localization schemes.

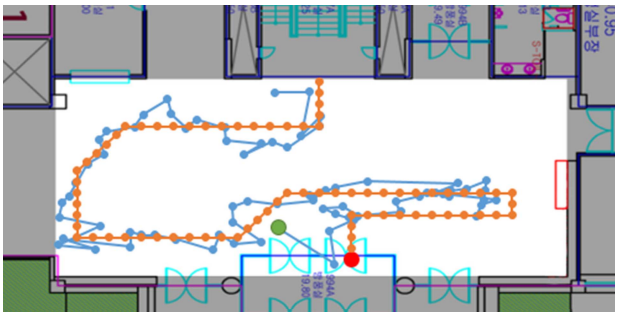

Fig. 12. Visualization of evaluation results for a sample path. The orange line shows the original path while the blue line shows a predicted path

Figure 13 shows the localization performance of the RNN model as we vary the number of hidden nodes from 10 to 50, 100, 200 and 300. The darkened thick box for each element in the figure represents the range where 75% of the total data set is collected while the line represents the range where 95% of the data is collected. As we increase the number of hidden nodes, we could generally improve the localization performance. However, we observe that the maximum error increases from 3.874m to 5.109m when we increase the number of hidden nodes from 200 to 300. This may be the result of overfitting of the model with 300 nodes.

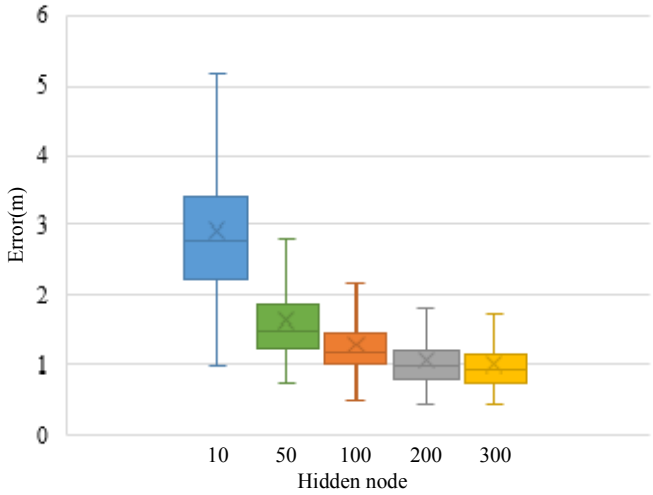

Fig. 13. Localization performance in terms of the number of hidden nodes

V. CONCLUSION

In this paper, we propose a new geomagnetic sensor based indoor localization scheme by using deep learning technique known as Recurrent Neural Network. From 1 million coordinate and sensor traces generated from the geomagnetic field map, we use 95% of the traces for training and 5% for evaluation. By optimizing the number of hidden nodes as well as other training parameters, we could achieve localization errors ranging from 0.441 to 3.874 meters for our test-bed. On average, we could achieve a localization accuracy of 1.062 meters, which substantially outperforms the existing RF-based indoor localization algorithms such as BLE fingerprinting [8]. In addition, we can also produce a smooth and continuous movement tracking results for pedestrian movement due to its accuracy as well as due to the characteristics of RNN whose output is not only based on its current input but also its previous inputs.

The geomagnetic field data have two distinct advantages over RF signal. First, the geomagnetic value of a single location is usually very stable unlike RF signal strengths since RF signal is vulnerable to reflection, diffusion, and scattering in indoor environment. Second, we can significantly reduce the cost of implementing localization infrastructure since we do not have to construct the indoor RF signal generating equipment such as access points or BLE beacons. This is because the movement of the Earth naturally produces the geomagnetic field both indoor and outdoor environment. Recently, there are various advanced RNN models such as LSTM [22] and bidirectional RNN. We plan to extend our work for a more large-scale commercial indoor environment by using the more advanced artificial neural network models through our future study.

REFERENCES

[1] Liu, H., Darabi, H., Banerjee, P., and Liu, J., "Survey of wireless indoor positioning techniques and systems," in *IEEE Transactions on SMC, Part C (Applications and Reviews)*, 37(6), 2007, pp. 1067-1080.

[2] Bahl, P., and Padmanabhan, V. N., "RADAR: An in-building RF-based user location and tracking system," in *Proceedings of the IEEE INFOCOM,* Vol. 2, 2000, pp. 775-784.

[3] Bahl, P., Padmanabhan, V. N., and Balachandran, A., "Enhancements to the RADAR user location and tracking system," in *Microsoft Research*, MSR-TR-2000-12, 2000, pp. 775-784.

[4] Ni, L. M., Liu, Y., Lau, Y. C., and Patil, A. P., "LANDMARC: indoor location sensing using active RFID," in *Wireless networks*, 10(6), 2004, pp. 701-710.

[5] An, J. H., & Choi, L., "Inverse fingerprinting: server side indoor localization with Bluetooth low energy," in *IEEE PIMRC,* 2016, pp. 1-6.

[6] Weissman, Z., "Indoor location," in *White paper*, Tadlys Ltd., 2004.

[7] Otsason, V., Varshavsky, A., LaMarca, A., and De Lara, E., "Accurate GSM indoor localization," in *UBICOMP,* 2005, pp. 141-158.

[8] Cheng, Y. C., Chawathe, Y., LaMarca, A., and Krumm, J., "Accuracy characterization for metropolitan-scale Wi-Fi localization," in *Proceedings of the 3rd ACM MOBISYS,* 2005, pp. 233-245.

[9] Brunato, M., and Battiti, R., "Statistical learning theory for location fingerprinting in wireless LANs," in *Computer Networks*, 47(6), 2005, pp. 825-845.

[10] Battiti, R., Le, N. T., and Villani, A., "Location-aware computing: a neural network model for determining location in wireless LANs," University of Trento, 2002.

[11] Youssef, M. A., Agrawala, A., and Shankar, A. U., "WLAN location determination via clustering and probability distributions," in *IEEE PERCOM,* 2003, pp. 143-150.

[12] Youssef, M., and Agrawala, A., "Handling samples correlation in the horus system," in *IEEE INFOCOM,* Vol. 2, 2004, pp. 1023-1031.

[13] Ladd, A. M., Bekris, K. E., Marceau, G., Rudys, A., Wallach, D. S., and Kavraki, L. E., "Using wireless ethernet for localization," in *IEEE IROS,* Vol. 1, 2002, pp. 402-408.

[14] Haeberlen, A., Flannery, E., Ladd, A. M., Rudys, A., Wallach, D. S., and Kavraki, L. E., "Practical robust localization over large-scale 802.11 wireless networks," in *Proceedings of the 10th annual ACM MOBICOM*, 2004, pp. 70-84.

[15] Haverinen, J., and Kemppainen, A., "Global indoor self-localization based on the ambient magnetic field," in *Robotics and Autonomous Systems*, *57*(10), 2009, pp. 1028-1035.

[16]. Friis, Harald T., "A note on a simple transmission formula," in Proceedings of the IRE 34.5, 1946, pp. 254-256.

[17] Shu, Y., Bo, C., Shen, G., Zhao, C., Li, L., and Zhao, F., "Magicol: indoor localization using pervasive magnetic field and opportunistic WiFi sensing," in *IEEE J-SAC*, 33(7), 2015, pp. 1443-1457.

[18] Chulliat, A., S. Macmillan, P. Alken, C. Beggan, M. Nair, B. Hamilton, A. Woods, V. Ridley, S. Maus and A. Thomson, "The US/UK World Magnetic Model for 2015-2020," in *Technical Report, National Geophysical Data Center*, NOAA, doi: 10.7289/V5TB14V7, 2015.

[19] Edwin Hall, "On a New Action of the Magnet on Electric Currents," in *American Journal of Mathematics*, 2 (3): 287–92, doi:10.2307/2369245, JSTOR 2369245, Archived from the original on 2011-07-27, Retrieved 2008-02-28, 1879

[20] Johnson, David B., and David A. Maltz, "Dynamic source routing in ad hoc wireless networks," in *Mobile computing,* 1996, pp. 153-181.

[21] Ioffe, S., and Szegedy, C., "Batch normalization: Accelerating deep network training by reducing internal covariate shift," *in ICML,* 2015.

[22] Hochreiter, S., and Schmidhuber, J., "Long short-term memory," in *Neural computation*, 9(8), 1997, pp. 1735-1780.